Scientific Visualization, 2023, volume 15, number 1, pages 71 - 82, DOI: 10.26583/sv.15.1.06

Computer and Physical Modeling for the Estimation of the Possibility of Application of Convolutional Neural Networks in Close-Range Photogrammetry

V.V. Pinchukov[1], A.Yu. Poroykov[2], E.V. Shmatko[3], N.Yu. Sivov[4]

National Research University "Moscow Power Engineering Institute"

[1] ORCID: 0000-0002-5816-0424 , vpinchukov@list.ru
[2] ORCID: 0000-0002-9284-1397 , poroykovay@gmail.com
[3] ORCID: 0000-0003-3565-9502, shmatko.97@bk.ru
[4] ORCID: 0000-0002-3120-7325, sivovny@mpei.ru

Abstract

Close-range photogrammetry is widely used to measure the surface shape of various objects and its deformations. The classic approach for this is to use a stereo pair of images, which are captured from different angles using two digital video cameras. The surface shape is measured by triangulating a set of corresponding two-dimensional points from these images using a predetermined location of cameras relative to each other. Various algorithms are used to find these points. Several photogrammetry methods use cross-correlation for this purpose. This paper discusses the possibility of replacing the correlation algorithm with neural networks to determine displacements of small areas in the images. They allow increasing the calculation speed and the spatial resolution of the measurement results. To verify the possibility of using convolutional networks for photogrammetry tasks, computer and physical modeling were carried out. For the first test, a set of synthetically generated images representing images of the Particle Image Velocimetry method was used. The displacements of particles in the images are known, it allows to estimate the accuracy of processing of such images. For the second test, a series of experimental images with surfaces with different deformation was obtained. Computational experiments were performed to process synthetic and experimental images using selected neural networks and a classical cross-correlation algorithm. The limitations on the use of the compared algorithms were determined and their error in reconstructing the three-dimensional shape of the surface was evaluated. Computer and physical modeling have shown the operability and efficiency of neural networks for processing photogrammetry images.

Keywords: Close-range photogrammetry, convolution networks, image pattern correlation technique, cross-correlation.

1. Introduction

Optical measurement methods are widely used in all fields of science and technology. Such methods include methods of close-range photogrammetry [1]. They allow measuring the shape of the object surface contactless with high spatial resolution and high accuracy over a large area. The basic principle of these methods is to obtain three-dimensional coordinates of the object from its two-dimensional images. The main approach for this is to use two digital video cameras. Two images of the same object obtained from different angles allow reconstructing three-dimensional coordinates of the object. To achieve this, it is necessary to determine the corresponding points on the images. For this purpose, various methods are used: algorithms for finding key (feature) points, structured illumination, epipolar geometry, cross-correlation analysis, etc.

One of the photogrammetry methods is based on cross-correlation processing of stereo pairs of images. It is an Image Pattern Correlation Technique (IPCT) [2-5]. It is based on processing algorithms of another method – Particle Image Velocimetry (PIV) [6] and is another variant of Digital Image Correlation method (DIC) [7].

In contrast, its universality, the method for finding corresponding points based on cross-correlation analysis has its disadvantages. The first of them is the proportional increasing of the calculation complexity with the increasing of the spatial resolution. The second is the direct dependence of the measurement error on the amplitude of the displacement of the corresponding points on the images. The greater the distance between the points, the greater the error. To reduce it, it is necessary to iteratively calculate the correlation function with decreasing aperture, which causes an increase in computational costs. In our work we attempted to apply machine learning methods to replace the cross-correlation calculation in the IPCT method to solve these problems.

Machine learning algorithms in PIV tasks have been used for a long time [8]. But due to the weak development of such an area as machine learning, this application was very limited and therefore was used only at the post-filtration stage. Since about 2012, there has been a greater interest in neural networks, namely convolutional neural networks, thanks to a successful solution proposed on ImageNet. Now this area has begun to develop actively again, not least because of the appearance of affordable and powerful GPUs, on which the execution and training of the network is much faster. One of the first proposals for the application of neural networks to PIV tasks was suggested in [9]. Since these were the first attempts in a new direction, the proposed ideas strongly intersected with cross-correlation algorithms. Two 32×32-pixel interrogation windows from two images were also uploaded to the network, and the network predicted the displacement vector corresponding to these windows. The first attempts [9], although they did not show better results compared to the already known methods, but they showed the efficiency of the idea, which was further developed. A similar study was conducted in [10], where a network with the architecture proposed in [11] was studied. Approaching modern solutions, we should mention the deep neural network from [12], which was used in [13] for PIV tasks, but with some modifications. The main one is a new database for training. More detailed methods of machine learning for diagnostic problems in hydrodynamics are given in [14-15].

In this work, two networks were used for the surface shape measurement problem: LiteFlowNet [16] and PIV-LiteFlowNet-en [17]. Both of these networks are successors of the FlowNet network [12], designed to receive two images at the input and evaluate the displacement of the optical flow at the output. According to [12], the network is trained on a large synthetic dataset and provides acceptable accuracy for estimating rigid motion. However, the original FlowNet cannot be directly applied to PIV problems, that was shown in [13].

2. Measurement techniques

2.1 Image Pattern Correlation Technique

Image Pattern Correlation Technique is an optical method of measuring the shape of a surface from its stereo images. The idea of IPCT, as in other photogrammetric methods, is to find the position of spatial points with unknown three-dimensional coordinates. For this purpose, two-dimensional coordinates of these points are searched for in two images registered with digital video cameras of stereo system. The determined coordinates allow calculating the required three-dimensional coordinates of the point with the help of triangulation procedure based on the known intrinsic and extrinsic parameters of the cameras.

IPCT uses a special pattern – a background pattern, usually represented by randomly distributed dots on a white background, or vice versa. Such a pattern allows to increase the contrast of the measured surface and significantly increases the efficiency of cross-correlation algorithm.

Cross-correlation processing of images consists of several consecutive steps. The first step is to divide the input images into small areas, the so-called interrogation windows, according to the specified parameters. Then a cross-correlation function is calculated for each pair of corresponding windows according to the formula

$$f(x,y) \circ g(x,y) = \int_{-\infty}^{\infty}\int_{-\infty}^{\infty} f^*(\eta,\xi)\cdot g(x+\eta, y+\xi)d\eta d\xi, \quad (1)$$

where $f(x, y)$ and $g(x, y)$ are two-dimensional functions of brightness distribution on images, $\circ$ – correlation operation, asterisk * – complex conjugation operation. Usually, calculation is performed using fast Fourier transform (FFT) algorithms, by the formula

$$f(x,y) \circ g(x,y) \Leftrightarrow F(u,v)^* G(u,v), \quad (2)$$

where $F(u, v)$ and $G(u, v)$ – Fourier images of $f(x, y)$ and $g(x, y)$. An additional advantage is achieved by calculating the normalized correlation function using the fast algorithm [18] using the formula

$$c_n(x,y) = c'(x,y)/\left[\sqrt{\sigma_1(x,y)}\sqrt{\sigma_2(x,y)}\right], \quad (3)$$

where $c`(x, y)$ – the correlation function of the transformed interrogation windows

$$f`(x,y) = f(x,y) - \mu_1, \quad g`(x,y) = g(x,y) - \mu_2$$

(μ_1, μ_2 – the average brightness value in the survey windows $f(x, y)$ and $g(x, y)$), obtained according to formula (2) using the FFT, and σ_1 и σ_2 – is the standard deviation of brightness in the interrogation windows, calculated as

$$\sigma_1(x,y) = \sum_{m=0}^{M}\sum_{n=0}^{N}(f(m,n)-\mu_1)^2, \quad (4)$$

$$\sigma_2(x,y) = \sum_{m=0}^{M}\sum_{n=0}^{N}(g(m,n)-\mu_2)^2. \quad (5)$$

The next step is to find the maximum for each calculated cross-correlation function with subpixel resolution by interpolating its peak. The most commonly used formula for approximating the maximum with a Gaussian function is

$$x`_{max} = x_{max} + [ln(c_{-1}) - ln(c_{+1})]/[2ln(c_{-1}) - 4ln(c_0) + 2ln(c_{+1})], \quad (6)$$

where $x`_{max}$ – approximated horizontal coordinate of the maximum; x_{max} – coordinate of the pixel with the maximum value of the correlation function; c_0, c_{-1} and c_{+1} – function values in the maximum and in the closest to it pixels with coordinates $x_{max} - 1$ и $x_{max} + 1$. Similarly, the coordinate of the maximum vertically $y`_{max}$.

The result of this algorithm is a vector field of point displacements on two images. It can be used to triangulate three-dimensional surface points directly. A single displacement vector with its origin defines the two-dimensional coordinates of the interrogation window center in the first image, and its end defines the two-dimensional coordinates in the second image. During triangulation of two-dimensional points, usually the pinhole camera model is used.

2.2 Neural networks

Many neural networks, which were considered when selecting specific candidates to be used in our work, have been implemented based on the Caffe library [19]. At the moment, their launch is associated with a lot of technical difficulties due to outdated code base. The LiteFlowNet-en and LiteFlowNet selected in the first section both have implementations on the PyTorch library [20], which allowed to successfully apply them for image processing.

An important feature of PIV-LiteFlowNet-en in contrast to LiteFlowNet is that at the output image it gives resolution equal to the input image without the use of bilinear interpolation, which increases the accuracy of small displacements.

Both networks require a CUDA-enabled GPU to run. The amount of video memory on the card is important, as it determines with whatresolution the image can be processed on the video card. In our work we used the service Google Colab [21], which allocates about 11 GiB of GPU memory per user, which allows us to process images of 1900×2000 pixels with a color depth of 24 bits. This is enough to process the experimental images used in this work at full resolution in the working area.

3. Research methods

3.1 Computer modeling

The first step in evaluating the possibility of using neural networks for photogrammetry was computer modeling. It consisted in processing the synthetic images using two selected networks and a standard cross-correlation algorithm [22]. The modeling evaluated the accuracy of determining the displacements on the synthetic images using different approaches. As test images the data set proposed in [13] was used. This set is a modeled PIV images of flows with different conditions and parameters. Details of the dataset and mean error for three tested algorithms are shown in Table 1. The result of modeling in form of the mean square error of the true flow (defined in the modeling) with the measured flow is shown in Figure 1. Processing by cross-correlation was performed using a software package of our own design [23]. Processing parameters: interrogation window size 24×24 pixels, interrogation window offset 4 pixels, approximation of correlation peak by Gaussian distribution.

Table 1. Image parameters in the dataset and computer modeling results

Case name	Description	Condition	Images quantity	PIV-Lite-FlowNet-en error, pixels	Lite-FlowNet error, pixels	Cross-correlation error, pixels
Back-step	Backward stepping flow	Re = 800 Re = 1000 Re = 1200 Re = 1500	600 600 1000 1000	0,043	0,155	0,292
Cylinder	Flow over a circular cylinder	Re = 40 Re = 150 Re = 200 Re = 300 Re = 400	50 500 500 500 500	0,202	0,315	0,312
DNS-turbulence	A homogeneous and isotropic turbulence flow	-	2000	0,204	0,589	0,783
JHTDB-channel	Channel flow	-	1900	0,080	0,218	0,311
JHTDB-channel hd	Forced isotropic turbulence	-	600	0,052	0,195	0,244
JHTDB-isotropic 1024 hd	Forced isotropic turbulence	-	2000	0,140	0,288	0,313
JHTDB-mhd 1024 hd	Forced MHD turbulence	-	800	0,090	0,349	0,382
SQG	Sea surface flow driven by SQG model	-	1500	0,203	0,652	0,875
Uniform	Uniform flow	Displacement 0÷5 pixels	1000	0,033	0,141	0,253

Figure 1 shows that the PIV-LiteFlowNet-en network has the best accuracy and small error variation for all flow cases considered. The LiteFlowNet network, which was not trained for PIV tasks, though has a large error, but shows good results, indicating its versatility for various applications. The cross-correlation method generally showed worse results, except for the "Cylinder" case, where it has a significant error variation. There is another disadvantage of cross-correlation processing – a vector field of lower density. While neural networks get a field of resolution equal to the size of the input image, for cross-correlation the field is 4 times less dense. This is due to the step between the interrogation windows of 4 pixels. But cross-correlation has the advantage that its calculation is executed entirely on the CPU, while neural networks need to use the GPU to achieve the processing speed advantage.

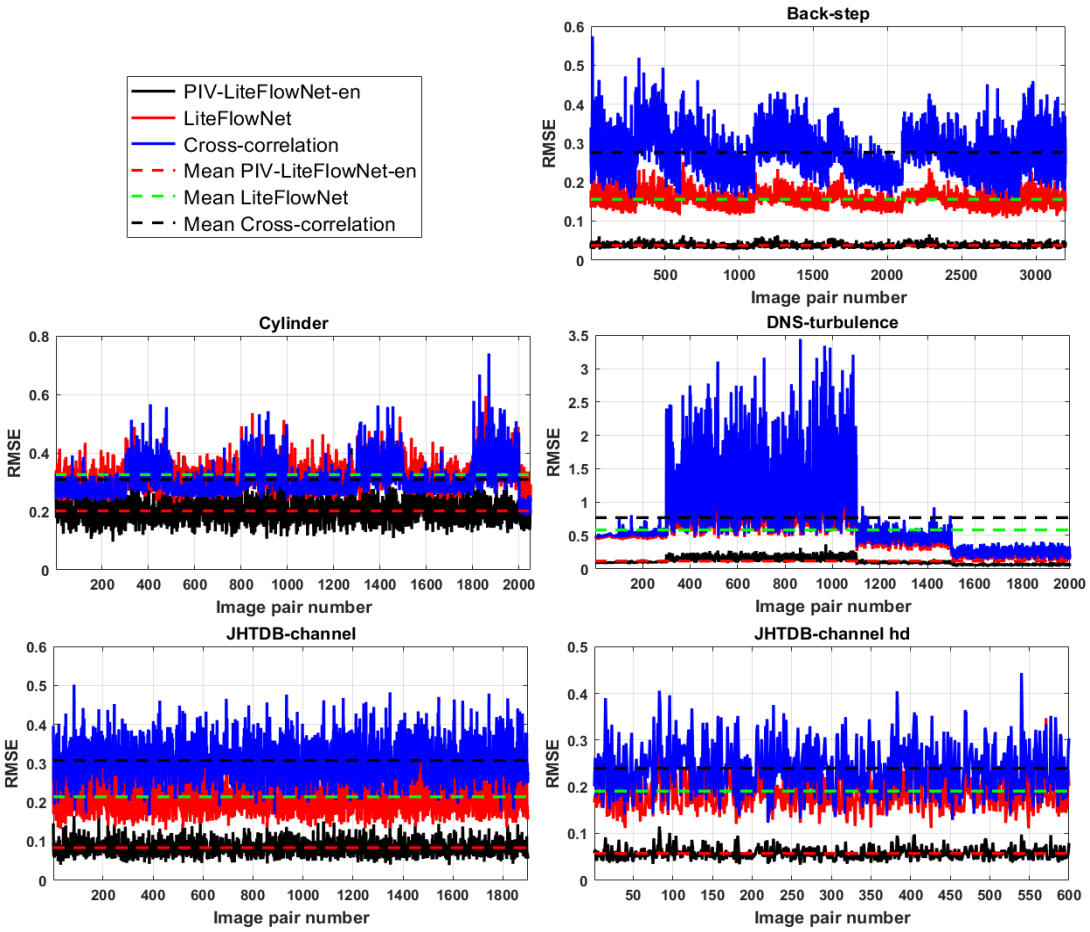

Figure 1. Results of computer modeling for two networks and cross-correlation

3.2 Physical modeling

To evaluate the results of processing by the compared algorithms with physical modeling, 150 pairs of experimental images of the surface with different deformations were used. The images were obtained using the imitator of deformable surface (IDS) described in [24]. The IDS allows to arbitrarily set the shape of the surface by means of digital servo-machines.

The IPCT method according to the algorithm described in [5] was used to reconstruct the surface shape. As pre-processing, the background pattern images were pre-matched using fiducial markers so, that the measured surface will be oriented perpendicularly to the optical axis of the camera. The size of each stereo pair was individual, but usually did not exceed 1700×1500 pixels. The second stage of image processing was a cross-correlation analysis (described in 2.1), which results were vector fields of surface point displacements between stereo pair images. The third stage was calculation of triangulation to determine three-dimensional surface coordinates. Figure 2 shows an example of stereo pair processing using PIV-LiteFlowNet-en. The results of perspective transformation are shown in Figure 2(c-d).

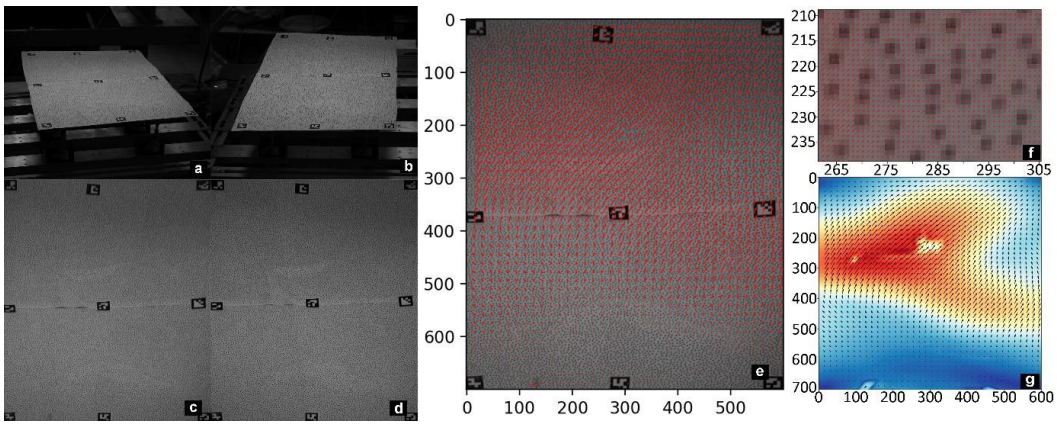

Figure 2. Example of stereo pair processing in experimental modeling, all samples measured in pixels: a, b – original images; c, d – results of perspective transformations; e – visualization of sparse vector field; f – visualization of vector field in full resolution; g – representation of deformation amplitude using color map

Before comparing the two selected networks and cross-correlation, it is necessary to determine the equivalent conditions for these algorithms. Figure 3 shows the vector fields for the same stereo pair, but at different resolutions of the image. Figure shows that the PIV-LiteFlowNet-en network cannot cope with offsets greater than ~12-13 pixels. For the LiteFlowNet network, this value is ~80-90 pixels.

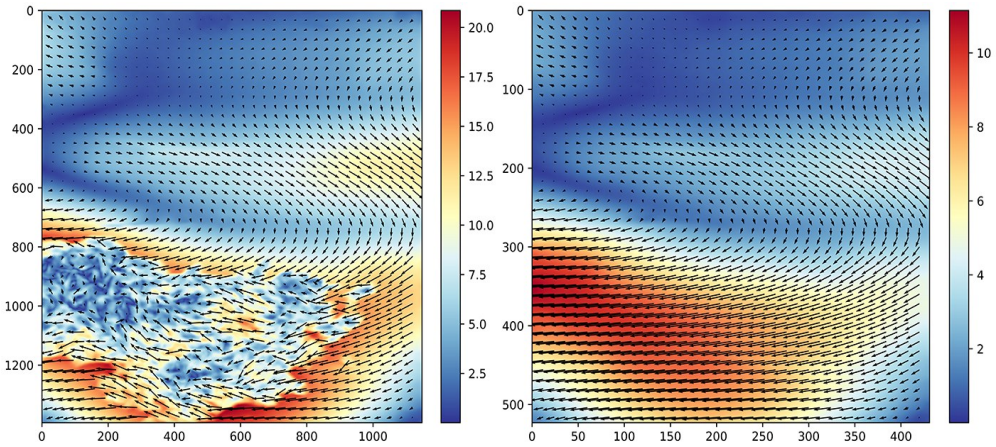
Figure 3. PIV-LiteFlowNet-en processing results for experimental images with different input image resolutions, colormap shows displacements in pixels

In order to compare networks with different ranges of measured displacements, it was decided to perform a calculation for images with different initial resolutions. In this case the displacements on the images will change proportionally to their size. This will allow comparing the results of the algorithms on the same experimental data. Calculation of the RMS of the reprojection error was performed for 10 resolutions of each experimental stereo pair. The series of resolutions used in the calculations was obtained by the following formula

$$R_k = R_0 - \frac{R_0}{10}k, \tag{7}$$

where k = 0,1,2...9; R_0 – the original size of the side of the image. In this case, the aspect ratio of the images is preserved. For the cross-correlation algorithm it was also necessary to define parameters for image processing. It was impossible to choose universal parameters, because the displacements can reach more than 100 pixels. Therefore, the size of the interrogation window must be determined individually for each resolution. The final processing parameters of the three tested algorithms are presented in Table 2.

Figure 4 shows the result of testing the three algorithms. Each curve is an average of 150 stereo pairs. In order to test the influence of the total intensity on the image, an inverse version of this pair was created on the basis of each pair of images. This is due to the fact that the IPCT method is characterized by black dots on a white background, while the PIV method is characterized by white dots on a black background.

Table 2. Image processing parameters with the algorithms being tested

Resolution, pixels	Interrogation window size, pixels	Step for interrogation window, pixels
1700×1500	256	128
1530×1350	256	128
1360×1200	196	98
1190×1050	196	98
1020×900	128	64
850×750	128	64
680×600	64	32
510×450	64	32
340×300	32	16
170×150	32	16

The following conclusions can be made from the processing results:

1. The cross-correlation algorithm shows a stable reprojection error for almost all resolutions. It is not affected by intensity inversion.

2. LiteFlowNet shows the best results among all the algorithms, while image inversion negatively affects its performance.

3. PIV-LiteFlowNet-en shows poor results due to large displacements in the images. At a resolution of 340×300 pixels, the displacements become quite small, but due to the high compression, the quality of the images does not allow the algorithm to achieve high accuracy. Image inversion improves the performance of the algorithm.

4. At 340×300 and 170×150 resolution, all algorithms show a decrease in accuracy due to strong image resizing.

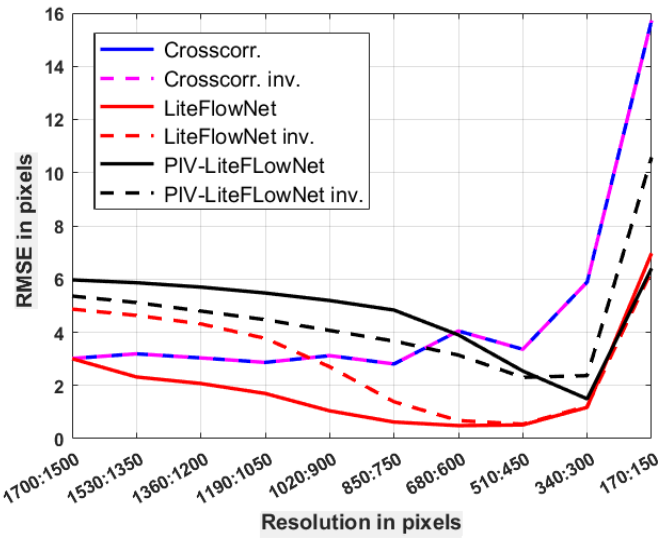

Figure 4. Average RMS value of the reprojection error for different resolutions for the three algorithms studied in physical modeling

To better understand the behavior of the algorithms, Figure 5 shows the RMS error for two stereo pairs: at small and large displacements in the images. Figure 5(a) shows graphs in the same plane for small and large displacements, 5(b) the value of this displacement for each resolution, 5(c) enlarged area 5(a), demonstrating the behavior of algorithms at small displacements. Comparing the graphs, we can once again see that the maximum estimated displacement of PIV-LiteFlowNet-en is about 10 pixels, and of LiteFlowNet about 80 pixels.

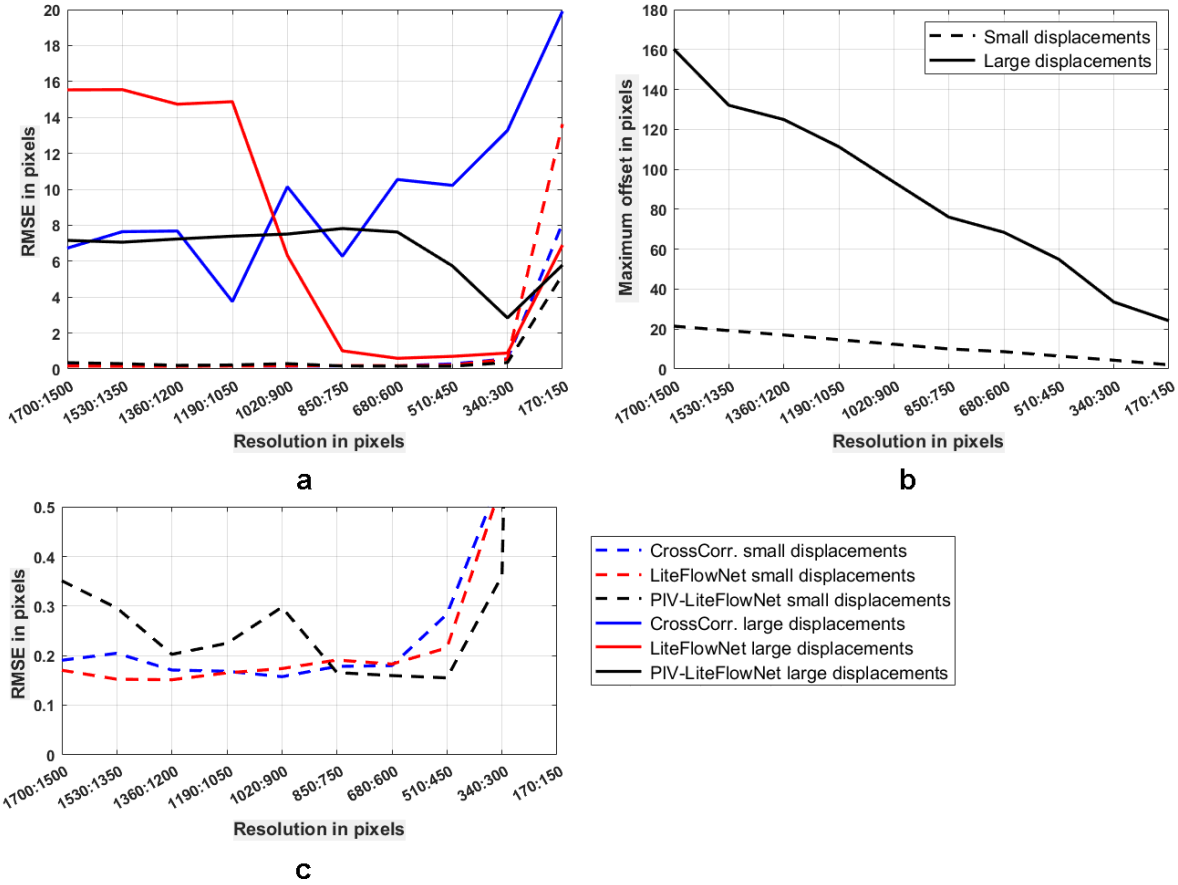

Figure 5. Average RMS value of the reprojection error for different displacement amplitudes in physical modeling: a – RMS of the reprojection error for small and large displacements; b – offset value for the two cases; c – enlarged area of the graph (a) to show the behavior of the algorithms at small displacements

For cross-correlation, the estimate of the maximum displacement depends on the size of the interrogation window. The maximum measured displacement should be less than 1/2 or 1/3 of the interrogation window size. From graphs 5(b) and 5(c) it can be seen that once the displacements in the images go down to 10 pixels or fewer, the PIV-LiteFlowNet-en network shows better results than the others, which further confirms the maximum estimated displacement. The average RMS of the reprojection error in Figure 5 for all algorithms is quite large, i.e., close to or greater than 1 pixel. This is explained by the fact that at large displacements, as in Figure 5, the error increases dramatically, which leads to increasing of the average error.

Based on the plots in Figure 5 the minimum error for PIV-LiteFlowNet-en is achieved at 510:450 resolution, for LiteFlowNet at 680:600. Figure 6 shows plots of reprojection error for each pair of images out of 150 taken. Also, the 850:750 and 1700:1500 resolutions are plotted for comparison. All graphs are sorted in order of increasing error for clarity. All plots, except for the 1700:1500 case, show the same patterns. The LiteFlowNet network has less error compared to the cross-correlation algorithm with approximately the same graph shape, only in a few cases does the cross-correlation exceed the accuracy of the network. The PIV-

LiteFlowNet-en network has the best accuracy of all the algorithms in about 50 cases. At the same time, it has a better performance in image inversion. The exception is the case at 510:450 resolution, where the accuracy for the image inversion case does not fall far behind the original images.

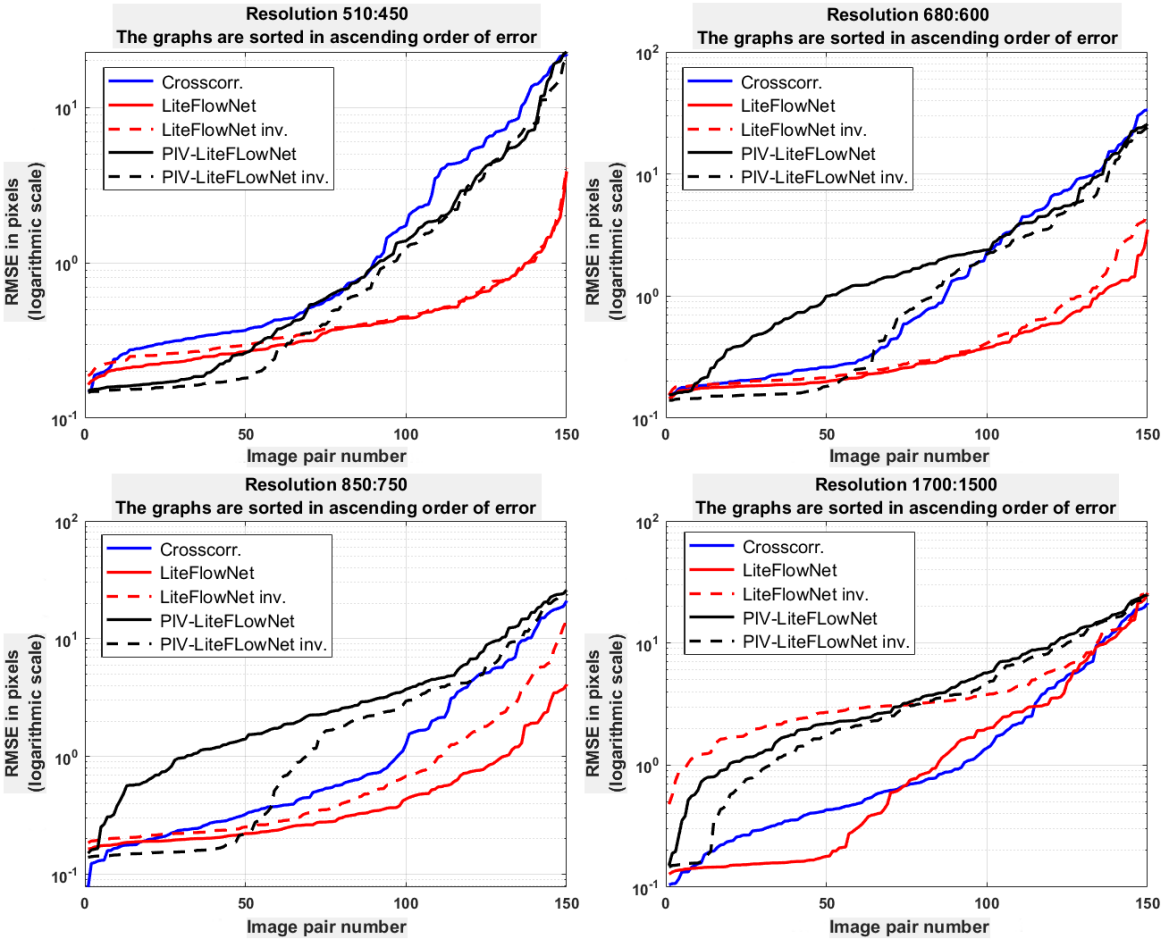

Figure 6. RMS error for each captured image pair for the three investigated algorithms at different resolutions in physical modeling

The fact that the PIV-LiteFlowNet-en network performs the best only in ~50 cases is due to the fact that even at 510:450 resolution, most image pairs have displacements greater than 10 pixels. Therefore, this network exceeds the other algorithms in only 1/3 of the cases. To demonstrate that none of the algorithms are able to process full resolution images with high accuracy, the case of 1700:1500 is given, which shows that acceptable accuracy is achieved by cross-correlation in about 10 cases and by LiteFlowNet in about 50 cases, which is not even half of the entire set. This is due to the large displacements in the images.

4. Conclusions

The paper describes the application of neural networks to the reconstruction of three-dimensional shape of the object surface by photogrammetry. The results of their processing were compared with the already proven algorithm based on cross-correlation. It allows estimating with an acceptable speed only the sparse vector field, by which three-dimensional points are calculated with triangulation. To find a solution to this problem, we reviewed machine learning methods, of which two neural networks LiteFlowNet and PIV-LiteFlowNet-en were selected. These networks allow estimating the vector field in full image resolution and at the same time have a higher calculation speed in comparison with cross-correlation. But the full gain in speed can be obtained only with the use of a graphics processor.

It was found that neural networks have a limit on the amount of correctly estimated displacement. For PIV-LiteFlowNet-en this limit was 12-13 pixels, and for LiteFlowNet about 80 pixels. For the first network, this can be explained by the training sample, and for the second by the network design. Also, the difference in the processing of original and inverse image networks was revealed, which is also a consequence of the training samples.

According to the processing results, LiteFlowNet exceeded the algorithm based on cross-correlation and PIV-LiteFlowNet-en in the sum for all image resolutions. But if we compare within the limitations of the algorithms, PIV-LiteFlowNet-en has better accuracy. At the same time, for processing images typical for photogrammetry in full resolution, none of the methods is satisfactory. For full application of such neural networks, their modification is required for the investigated task.

Conducted physical modeling to check selected approaches to image processing for photogrammetry problem showed their performance and efficiency. But it is necessary to solve several problems for their application in practice. The selected neural networks are not fully suitable for the problem under study due to the limitation of the estimated displacement value and high complexity of their running. For successful practical application of machine learning it is necessary to modify the design of selected neural networks, or to develop their own design, and to train them on experimental images, specific to photogrammetry.

Acknowledgements

The investigation has been carried out within the framework of the project “Development of a machine vision system for determining the position of objects in space based on fiducial markers” with the support of a subvention from the National Research University “MPEI” for implementation of the internal research program “Priority 2030: Future Technologies” in 2022-2024.

References

[1] Luhmann T., Robson S., Kyle S., Boehm J. Close-range photogrammetry and 3D imaging // Close-Range Photogrammetry and 3D Imaging, de Gruyter, 2019. 708 p. (doi:10.1515/9783110607253)

[2] Meyer R., Kirmse T., Boden F. Optical in-flight wing deformation measurements with the image pattern correlation technique // New Results in Numerical and Experimental Fluid Mechanics IX. Springer, Cham, 2014. Vol. 124. Pp. 545–553. (doi:10.1007/978-3-319-03158-3_55)

[3] Kirmse T. Recalibration of a stereoscopic camera system for in-flight wing deformation measurements // Meas. Sci. Technol., 2016. Vol. 27. № 5. P. 54001. (doi:10.1088/0957-0233/27/5/054001)

[4] Boden F., Lawson N., Jentink H.W., Kompenhans J. Advanced In-Flight Measurement Techniques, 2013. 344 p. (doi: 10.1007/978-3-642-34738-2)

[5] Poroykov A.Yu., Surkov D.A., Ulyanov D.B., Ilyinac N.S., Shmatko E.V., Pinchukov V.V. Development of an on-board measuring system for diagnosing deformation of aerodynamic surfaces in a flight experiment // Journal of communications technology and electronics, 2021. Vol. 66. № 11. Pp. 1274–1281. (doi:10.1134/S1064226921110073)

[6] Raffel M., Willert C.E., Scarano F. et al. Particle Image Velocimetry: A Practical Guide // Berlin: Springer, 2018. 669 p. (doi:10.1007/978-3-319-68852-7)

[7] Schreier H., Orteu J.-J., Sutton M.A. Image Correlation for Shape, Motion and Deformation Measurements // Springer: New York, NY, USA, 2009. 322 p. (doi:10.1007/978-0-387-78747-3)

[8] Grant I., Pan X. The use of neural techniques in PIV and PTV // Meas. Sci. Technol., 1997. Vol. 8. №. 12. Pp. 1399–1405. (doi:10.1088/0957-0233/8/12/004)

[9] Rabault J., Kolaas J., Jensen A. Performing particle image velocimetry using artificial neural networks: a proof-of-concept // Meas. Sci. Technol., 2017. Vol. 28. №12. P. 125301. (doi:10.1088/1361-6501/aa8b87)

[10] Lee Y., Yang H., Yin Z. PIV-DCNN: cascaded deep convolutional neural networks for particle image velocimetry // Experiments in Fluids, 2017. Vol. 58. № 12. P. 171. (doi:10.1007/s00348-017-2456-1)

[11] Sun Y., Wang X., Tang X. Deep Convolutional Network Cascade for Facial Point Detection // 2013 IEEE Conference on Computer Vision and Pattern Recognition, 2013. Pp. 3476–3483. (doi:10.1109/CVPR.2013.446)

[12] Dosovitskiy A. et al. FlowNet: Learning Optical Flow with Convolutional Networks // 2015 IEEE International Conference on Computer Vision (ICCV), 2015. Pp. 2758–2766. (doi:10.1109/ICCV.2015.316)

[13] Cai S., Zhou Sh., Xu Ch., Gao Q. Dense motion estimation of particle images via a convolutional neural network // Experiments in Fluids, 2019. Vol. 60. №. 73. (doi:10.1007/s00348-019-2717-2)

[14] Brunton S.L., Noack B.R., Koumoutsakos P. Machine learning for fluid mechanics // Annual review of fluid mechanics, 2020. Vol. 52. Pp. 477–508. (doi:10.1146/annurev-fluid-010719-060214)

[15] Znamenskaya I.A. Methods for Panoramic Visualization and Digital Analysis of Thermophysical Flow Fields. A Review. // Scientific Visualization, 2021. Vol. 13. № 3. Pp. 125–158. (doi:10.26583/sv.13.3.13)

[16] Gim Y., Jang D.K., Sohn D.K., Kim H., Ko H.S. Three-dimensional particle tracking velocimetry using shallow neural network for real-time analysis // Experiments in Fluids, 2020. Vol. 61. P. 26. (doi:10.1007/s00348-019-2861-8)

[17] Cai S., Liang J., Gao Q., Xu C., Wei R. Particle Image Velocimetry Based on a Deep Learning Motion Estimator // IEEE Transactions on Instrumentation and Measurement, 2020. Vol. 69. № 6. Pp. 3538–3554. (doi:10.1109/TIM.2019.2932649)

[18] Yoo J. C., Han T.H. Fast Normalized Cross-Correlation // Circuits, systems and signal processing, 2009. Vol. 28. №. 6. P. 819. (doi: 10.1007/s00034-009-9130-7)

[19] Caffe | Deep Learning Framework [Electronic resource] URL: https://caffe.berkeleyvision.org (accessed 16.11.2022).

[20] PyTorch [Electronic resource] URL: https://pytorch.org (accessed 16.11.2022).

[21] Google Colab [Electronic resource] URL: https://colab.research.google.com (accessed 16.11.2022).

[22] Pinchukov V.V., Poroykov A.Yu., Shmatko E.V., Bogachev A.D., Sivov N.Yu. Comparison of the neural networks with cross-correlation algorithm for the displacements on images estimation // 2022 Wave Electronics and its Application in Information and Telecommunication Systems (WECONF), 2022. Pp. 1–5. (doi:10.1109/WECONF55058.2022.9803453)

[23] Shmatko E.V., Pinchukov V.V., Bogachev A.D., Poroykov A.Yu. Crosscorrelation image processing for surface shape reconstruction using fiducial markers // Journal of Physics: Conference Series, 2021. Vol. 2127. P. 012030. (doi:10.1088/1742-6596/2127/1/012030)

[24] Ivanova Y.V., Poroykov A.Y. Estimation of the measurement error of photogrammetric techniques by controlled flexible deformable surface // 2019 International Youth Conference on Radio Electronics, Electrical and Power Engineering (REEPE), IEEE, 2019. Pp. 1–5. (doi:10.1109/REEPE.2019.8708779)